

## Article

# Therapeutic Potential of Cancer Vaccine Based on MHC Class I Cryptic Peptides Derived from Non-Coding Regions

Serina Tokita<sup>1,2</sup>, Takayuki Kanaseki<sup>1,\*</sup> and Toshihiko Torigoe<sup>1</sup> 

<sup>1</sup> Department of Pathology, Sapporo Medical University, Sapporo 060-8556, Japan; st.tokita@gmail.com (S.T.); torigoe@sapmed.ac.jp (T.T.)

<sup>2</sup> Sapporo Dohto Hospital, Sapporo 065-0017, Japan

\* Correspondence: kanaseki@sapmed.ac.jp; Tel.: +81-11-611-2111 (ext. 49981); Fax: +81-11-643-2310

**Abstract:** MHC class I molecules display intracellular peptides on cell surfaces to enable immune surveillance under pathological conditions. The source of MHC class I antigens responsible for cancer protection is not fully understood. Here, we explored the MHC class I peptidome in mouse colon cancer cells using a proteogenomic approach. We showed that cryptic peptides derived from unconventional short open reading frames accounted for part of the MHC class I peptidome. Moreover, cancer growth was significantly prevented in mice immunized with a cocktail of synthesized cryptic peptides. Together, our data showed that the source of cancer antigens was not limited to fragments of consensus proteins. Cryptic antigens were displayed by MHC molecules and mediated anti-cancer effects, suggesting their therapeutic potential for cancer prevention.

**Keywords:** tumor immunotherapy; tumor antigen; MHC; cryptic peptide



**Citation:** Tokita, S.; Kanaseki, T.; Torigoe, T. Therapeutic Potential of Cancer Vaccine Based on MHC Class I Cryptic Peptides Derived from Non-Coding Regions. *Immuno* **2021**, *1*, 424–431. <https://doi.org/10.3390/immuno1040030>

Academic Editor: Niels Schaft

Received: 13 October 2021

Accepted: 4 November 2021

Published: 9 November 2021

**Publisher's Note:** MDPI stays neutral with regard to jurisdictional claims in published maps and institutional affiliations.



**Copyright:** © 2021 by the authors. Licensee MDPI, Basel, Switzerland. This article is an open access article distributed under the terms and conditions of the Creative Commons Attribution (CC BY) license (<https://creativecommons.org/licenses/by/4.0/>).

## 1. Introduction

Cytotoxic CD8<sup>+</sup> T cells can eliminate malignant and virally infected cells. They perform immune surveillance by monitoring antigen peptides displayed by MHC class I molecules to detect abnormalities or changes in target cells. Susceptibility to immune checkpoint inhibitors (ICIs), observed in a variety of cancer types with mismatch-repair deficiency, strongly suggests that MHC molecules present mutation-derived neoantigens and that these antigens play a role in cancer rejection, mediated by cytotoxic CD8<sup>+</sup> T cells [1,2]. However, the majority of neoantigens are private antigens derived from passenger mutations, and the presentation of neoantigens is most likely to occur in a limited number of cancers with a high tumor mutation burden (TMB) [3]. Despite the fact that immunogenic neoantigens can induce reactive T cell responses and mediate cancer rejection [4], the specificity of current in silico prediction methods for selecting immunogenic neoantigens from an array of somatic mutations is not satisfactory, hindering the therapeutic use of these antigens in clinical settings.

Peptides displayed by MHC class I are generated by the intracellular antigen processing machinery. A variety of protein fragments digested by the proteasomes in the cytosol are transported into the endoplasmic reticulum, selected, customized, and ultimately loaded onto MHC class I molecules [5,6]. Thus, a peptide-MHC class I repertoire represents fragments of most, if not all, proteins generated inside the cell. However, the source of MHC class I peptides is not fully understood, and the discovery of a novel class of cancer antigens may create a breakthrough in immunotherapy. MHC class I peptides potentially arise from unconventional translation products that are separate from the known proteome [7,8]. Proteogenomic analyses have enabled the direct identification of cryptic peptide sequences and demonstrated that MHC-class I peptides originate from unconventional open reading frames (ORFs) in human tumor tissues [9–11]. A seminal study reported that MHC molecules presented tumor-associated antigens, derived from noncoding regions, that played protective roles in a mouse hematologic tumor model [12].

Recently, we identified an immunogenic cancer antigen derived from an oncogenic long non-coding RNA (lncRNA) in human colorectal cancer tissues [13]. CD8<sup>+</sup> T cell responses against this antigen and its MHC presentation were observed in multiple patients. Here, we hypothesized that some cryptic peptides, if not all, are aberrantly present in cancer cells, serving as cancer antigens. These unexplored antigen types may serve as targets for cancer immunotherapy, regardless of the TMB. In this study, we aimed to identify cryptic peptides in the MHC class I peptide repertoire of mouse colon cancer cells, and comprehensively assess their potential as the basis of a vaccine for preventing solid cancer growth.

## 2. Results

### 2.1. Direct Detection of Cryptic Peptides Presented by MHC Class I Molecules in Mouse Colon Cancer Cells

To comprehensively capture the MHC class I peptidome, including cryptic peptides derived from allegedly noncoding ORFs, we employed a proteogenomic approach that combined mass spectrometry (MS) sequencing with transcriptomic data (Figure 1A). Peptide-H-2D<sup>d</sup> complexes were immunoprecipitated from the cell lysate of CT26, a mouse colon cancer line, using a specific antibody, and the eluted D<sup>d</sup>-bound peptides were subsequently analyzed using MS. The MS spectra were searched against a custom reference database, which contained the computationally translated sequences of any potential ORFs in the mouse transcripts registered in the GENCODE ([www.genencodegenes.org](http://www.genencodegenes.org)). Matched sequences with a false discovery rate (FDR) of 0.01 were pooled, and D<sup>d</sup>-bound peptide candidates were selected based on the multiple factors: peptide length, NetMHC affinity score, and expression of the peptide-encoding gene in CT26 cells. The resulting sequences were searched against the UniProtKB database ([www.uniprot.org](http://www.uniprot.org)). Sequences not registered in the proteome database were classified as cryptic MHC peptides. This proteogenomic pipeline yielded 534 unique H-2D<sup>d</sup>-bound peptide sequences comprising 514 canonical and 20 cryptic peptides (Figure 1B). Cryptic peptides accounted for 3.75% of the H-2D<sup>d</sup>-bound peptidome.

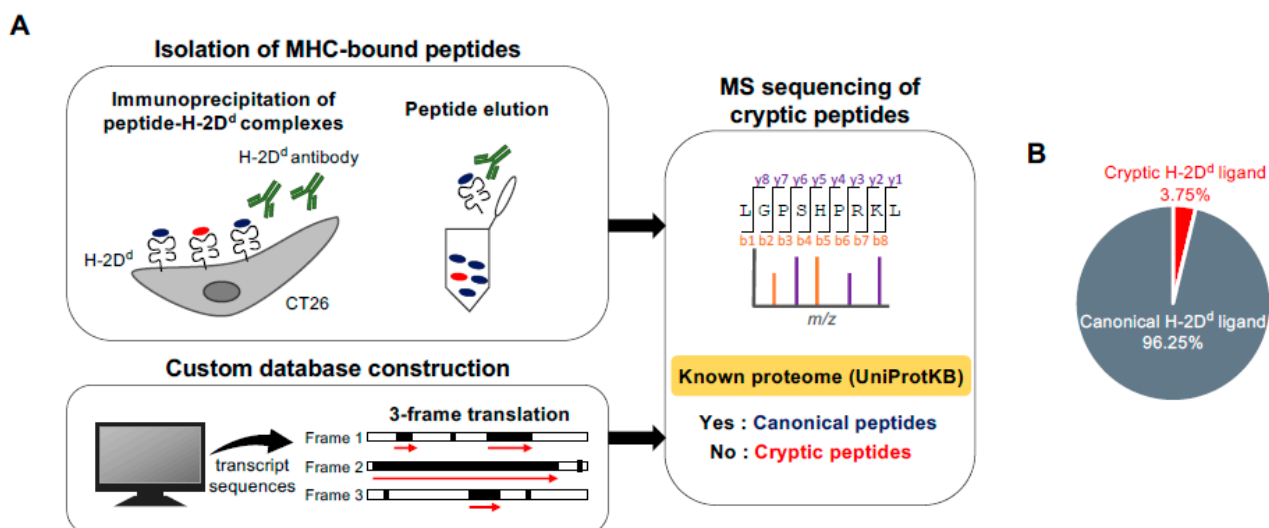


**Figure 1.** Proteogenomic pipeline for cryptic MHC class I peptide identification. (A) Peptide-MHC class I complexes were isolated from cell lysates using an H-2D<sup>d</sup>-specific antibody, and the eluted peptides were analyzed by MS. The MS spectra were searched against a custom reference database containing not only consensus protein sequences but also computationally translated products from any possible ORFs. The matched peptide sequences were then searched against the UniProtKB database and classified as canonical or cryptic MHC class I peptides. (B) Pie chart showing the proportion of cryptic peptides in the H-2D<sup>d</sup> peptidome of CT26 cells ( $n = 534$ ).

## 2.2. Characterization of MHC Class I Cryptic Peptidome

Both canonical and cryptic peptides had known characteristics of H-2D<sup>d</sup>-binding peptides: 9-mer sequences were dominant in terms of length, and Gly, Pro, and Leu/Phe/Ile, consensus H-2D<sup>d</sup>-binding anchor motifs, were conserved at positions 2, 3, and 9 (Figure 2A,B). There was also a trend shared between canonical and cryptic peptides: both types of peptides originated from abundantly expressed genes (Figure 2C). The majority of the source genes encoding the cryptic peptides were annotated as protein coding in GENCODE, as they contained at least one transcript harboring a consensus ORF for protein translation. However, the ORFs encoding cryptic peptides were found in different reading frames. Cryptic peptides were distinct from canonical peptides in terms of ORF lengths; the average ORF length of cryptic peptides was significantly shorter than that of canonical peptides (Figure 2D).

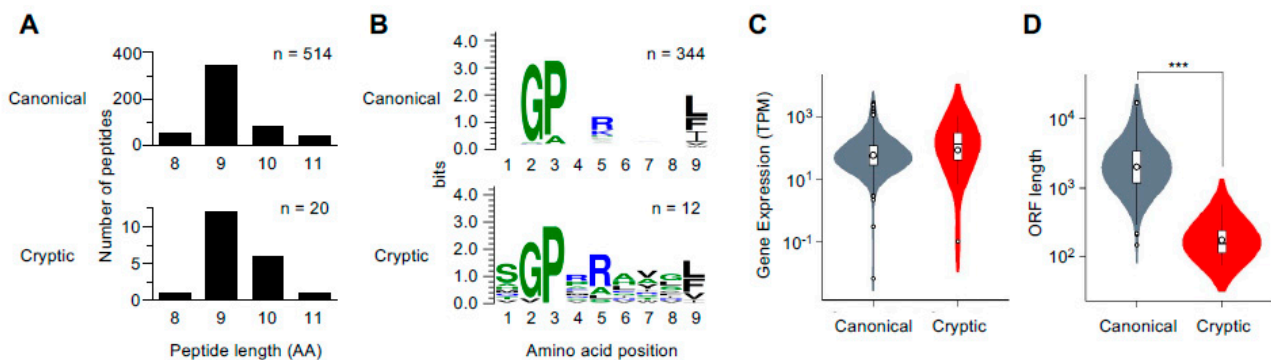


**Figure 2.** Characterization of MHC class I peptidome consisting of canonical and cryptic peptides. (A,B) Peptide lengths (A) and logo sequences (B) of the canonical and cryptic peptides identified in this study. (C) Violin plots showing the expression levels of the source genes encoding canonical and cryptic H-2D<sup>d</sup> peptides. (D) Comparison of the lengths of ORFs responsible for canonical and cryptic H-2D<sup>d</sup> peptide translation. *p*-values were calculated using a two-tailed unpaired Welch's *t*-test (\*\*\*) *p* < 0.001).

## 2.3. Vaccination with Cryptic MHC Class I Peptides Prevented Cancer Growth In Vivo

Next, we assessed the therapeutic potential of the identified cryptic peptides for preventing tumor growth in vivo. Although it is possible to predict the cancer specificity of each cryptic peptide to optimize the candidate peptide pools, we chose to test all 20 identified peptides (19 non-overlapping peptides) to avoid the risk of false-negative exclusion of immunogenic peptides. The peptides were synthesized and divided into seven groups, each containing 1–3 cryptic peptides (Table 1). The synthetic peptide cocktails were subcutaneously injected into BALB/c mice along with adjuvants, followed by CT26 cancer cell injection, and tumor growth was periodically measured (Figure 3A). In six of the seven groups, the sizes of the challenged tumors were not statistically different between the vaccinated and control groups injected with the adjuvant alone (Figures 3B and S1A,B). Interestingly, tumor growth was significantly prevented in mice injected with Group 6 peptides. This group contained three cryptic peptides derived from the *Ndrp1*, *Mrps18b*, and *Lonp1* genes. Similar to other cryptic peptides, their epitope sequences originated from shorter ORFs, independent of the consensus protein-coding ORFs (Figure 3C).

**Table 1.** Cryptic H-2D<sup>d</sup> peptides identified in CT26 cells.

	Sequence	Symbol	Length	Source Gene	GENCODE Gene Type	Gene Expression in CT26 (TPM)	NetMHC4.0 Score (IC <sub>50</sub> )
Group 1	MGPPRAAGI	MI9	9	1110038B12Rik	lncRNA	379.93	769.7
Group 2	AGPVAVSRF	AF9	9	Spr	Protein coding	104.78	4099.2
Group 2	QGPDRGGDSL	QL10	10	Ss18l2	Protein coding	41.72	983.1
Group 2	HGPRLEISL	HL9	9	Ythdf3	Protein coding	38.36	650.9
Group 3	SGPARAWGV	SV9	9	Poli	Protein coding	16.49	2567.1
Group 3	SGPSRLYLL	SL9	9	Rpl3	Protein coding	1107.39	196.4
Group 3	TGPVRLSVF	TF10	10	Sdhd	Protein coding	131.92	272.2
Group 4	QPARYFGF	QF8	8	Paics	Protein coding	272.20	3627.6
Group 4	SVPRRHVSF	SF9	9	Phlda3	Protein coding	206.73	497.8
Group 4	RGPERSEETVF	RF11	11	Plagl2	Protein coding	18.95	243.3
Group 5	SGPRSIYIL	SL9	9	Kcnb1	Protein coding	0.11	368.3
Group 5	LGPARSSSF	LF10	10	Lig4	Protein coding	6.86	453.9
Group 5	RGPVAGAVGL	RL10	10	Lonp1	Protein coding	298.21	3394.3
Group 6	SGPLRGAGF	SF9	9	Lonp1	Protein coding	298.21	609.9
Group 6	SGPERHVFV	SV9	9	Mrps18b	Protein coding	137.11	381.5
Group 6	VGPPRATVL	VL9	9	Ndr1	Protein coding	871.65	203.3
Group 7	QGPMALRLF	QF9	9	Ciao2a	Protein coding	68.09	1517.8
Group 7	SGPSRWKHQM	SM10	10	Ephx1	Protein coding	242.73	4854.4
Group 7	TGPQRNVCL	TL9	9	Ip6k1	Protein coding	45.57	79.0

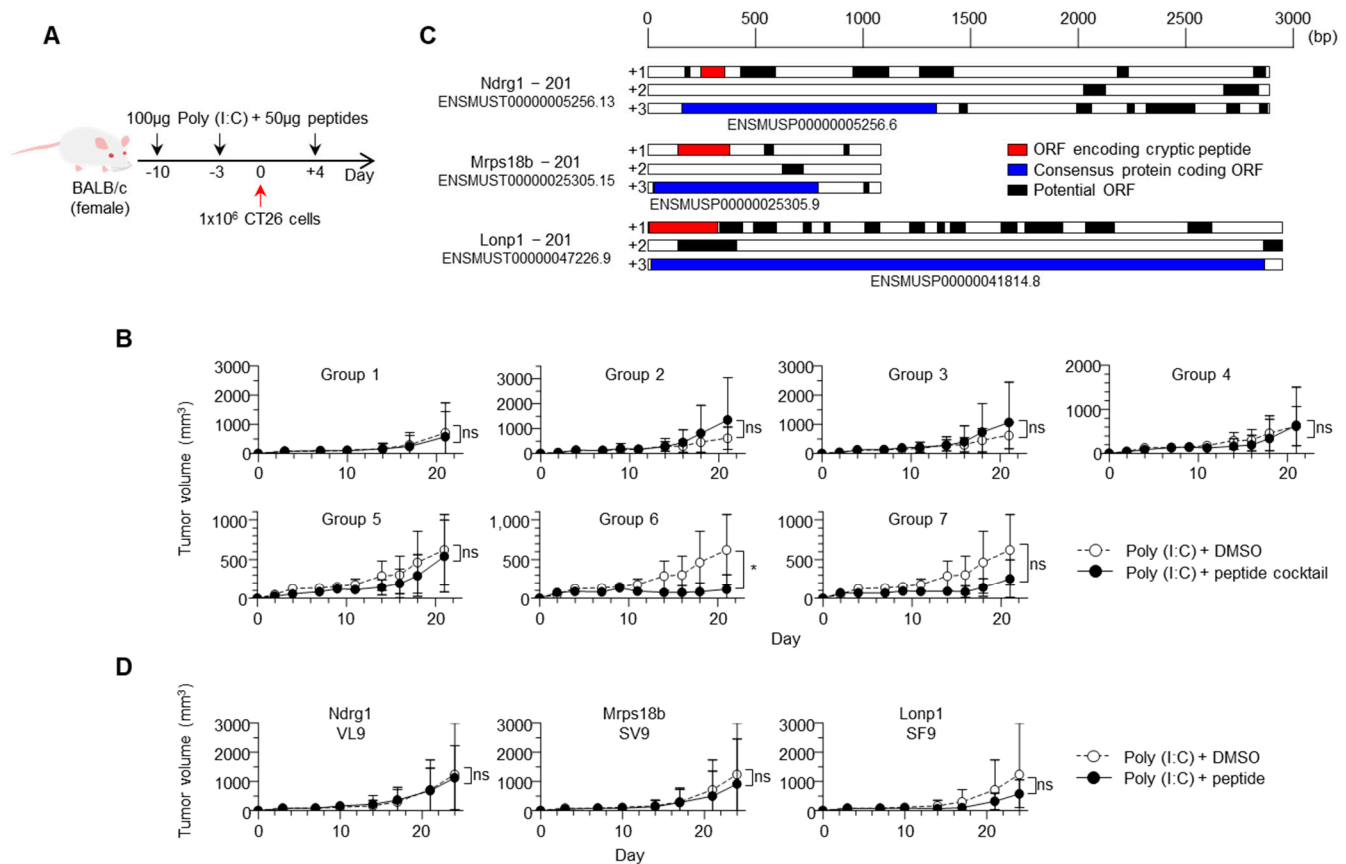


**Figure 3.** Vaccination with a cocktail of cryptic peptides prevented the growth of CT26 cells in vivo. **(A)** Schedule and dose of cryptic peptide vaccination (s.c.) and tumor injection in BALB/c mice. **(B)** Development of CT26 cells after cryptic peptide cocktail vaccination. Data represent the mean ± SD (*n* = 4 for Group 5; *n* = 5 for the other groups and the controls),

and  $p$ -values were calculated using a two-tailed  $t$ -test (\*  $p = 0.0485$ ). (C) Schematic representation of the transcripts encoding the cryptic peptides in Group 6. Black boxes indicate potential ORFs. Red and blue boxes indicate the ORFs encoding the cryptic H-2D<sup>d</sup> peptides and consensus protein sequences, respectively. (D) Development of CT26 cells after cryptic peptide vaccination. Here, three cryptic peptides in Group 6 were each administrated as a vaccine independently. Data represent the mean  $\pm$  SD ( $n = 5$ ), and  $p$ -values were calculated using a two-tailed  $t$ -test.

We also vaccinated mice with each of the three peptides independently and assessed tumor growth. Statistical differences were not observed, although the average tumor size was reduced as a result of the *Mrps18b* and *Lonp1* peptide vaccinations (Figures 3D and S1B). This result suggested that the anti-cancer effects induced by single peptide-based vaccines were insufficient, while induced T cells with different antigen specificities synergized when the peptides were administered simultaneously, possibly indicating the advantage of cocktail vaccination. Taken together, these results demonstrated the potential of cryptic peptides presented by MHC class I molecules to confer cancer protection.

### 3. Discussion

Cancer vaccines are a long sought-after therapeutic approach that induces specific T cell responses to prevent tumor growth. In contrast to ICI, which can be performed without knowledge of T cell antigen specificity, vaccination requires information about cancer antigens, ideally epitope sequences specifically presented by targeted tumor cells [14]. Recent technological advances in MS have enabled the capture of the MHC class I peptidomes of cancer cells, including mutation-derived neoantigens and cryptic antigens derived from allegedly noncoding regions. In this study, we explored the MHC class I peptidome of mouse colon cancer cells and found that cryptic peptides derived from noncoding regions accounted for up to 4% of the peptidome. Moreover, the growth of colon cancer was prevented in mice vaccinated with a peptide cocktail consisting of cryptic peptides derived from the *Ndrp1*, *Mrps18b*, and *Lonp1* genes. Anti-cancer effects mediated by these cryptic peptides were a surprise, since it is likely that cryptic peptide presentation itself is not always a cancer-specific event but also observed in normal tissues [13]. Our results support the previous finding that noncoding regions are a rich source of tumor-rejection antigens, even in solid cancers [12].

The intrinsic factors conferring immunogenicity to Group 6 cryptic peptides remain unclear. The induction of anti-cancer effects by vaccination may imply that cryptic translation events in cancer cells are upregulated compared with those in normal host tissues [15]. At least, these three genes were abundantly expressed in CT26 cells, based on transcriptome data. In our experiments, anti-cancer effects were observed when the vaccine containing all three peptides was administered. The effects were compromised when three peptides were administrated independently. It is well known that the ratio of tumor-reactive T cells to cancer cells (E/T) influences anti-tumor effects. Targeting multiple antigens may have induced a larger number of tumor-reactive T cells in total, which led to tumor rejection. According to this scenario, further optimization of T cell induction (e.g., an amount, dose, or route of peptide vaccination) may recover the anti-cancer effects. Alternatively, the simultaneous induction of three different TCRs with different antigen specificities may have prevented an escape from T cells due to antigen losses [16].

The screening for cryptic antigens in this study was limited to H-2D ligands, potentially excluding immunogenic peptides bound to MHC molecules of other classes. We note that none of the three peptide sequences have been reported in previous studies using the CT26 line. This is presumably attributable to different sensitivities in each proteogenomic pipeline; for instance, we focused on H-2D ligands and implemented direct immunoprecipitation using a specific antibody. Proteogenomic approaches have enabled analysis not only in cell lines but also in patient tissues; however, these approaches vary methodologically among most laboratories in terms of the biochemical isolation of MHC-bound peptides, construction of customized reference databases, and types of analysis software, requiring the laborious validation of identified sequences. The establishment of an efficient, standard method based on sample type should be further considered.

The discovery of cancer antigens that originate from noncoding regions and mediate tumor rejection in mice expands the pool of target antigens used for cancer immunotherapy in clinical settings. In contrast to mutation-derived neoantigens, cryptic peptides are unlikely unique to individual patients and may be related to tumorigenesis [13]. In summary, although the underlying mechanisms of tumor-oriented transcription and translation remain unclear, our data suggest the possibility of using cryptic peptides as new therapeutic targets.

## 4. Methods

### 4.1. Cell Line and Culture

The CT26 cell line (CRL-2638, ATCC) was cultured in complete RPMI1640 (Nacalai Tesque) supplemented with 10% FBS, 1% penicillin-streptomycin (Thermo Fisher Scientific, Tokyo, Japan), 1% GlutaMAX (Thermo Fisher Scientific), 10 mM HEPES (Thermo Fisher Scientific), 1 mM sodium pyruvate (Thermo Fisher Scientific), and 55  $\mu$ M 2-mercaptoethanol (Thermo Fisher Scientific) in a 5% CO<sub>2</sub> incubator at 37 °C. CT26 cell line was frozen in batches on arrival and not cultured over the maximum period of 8 weeks.

### 4.2. MHC Ligand Isolation and MS Analysis

To prepare the H-2D<sup>d</sup> mAb, 34-5-8S hybridoma (HB-102, ATCC) was cultured in Hybridoma serum free medium (Gibco) supplemented with 1% penicillin-streptomycin in CELLLine Bioreactor Flasks (CL1000, Corning). Condensed mAbs were collected and purified using HiTrap Protein G HP (GE Healthcare). Approximately  $1.2 \times 10^9$  CT26 cells were ground under cryogenic conditions and lysed with lysate buffer containing 0.25% sodium deoxycholate, 0.2 mM iodoacetamide, 1 mM EDTA, protease inhibitor cocktail (P8340, Sigma), 1 mM PMSF, and 1% octyl- $\beta$ -D glucopyranoside (Dojindo) in DPBS. The peptide-H-2D<sup>d</sup> complexes were captured using affinity chromatography of H-2D<sup>d</sup> mAb coupled to CNBr-activated Sepharose 4B (GE Healthcare) overnight. The MHC ligands were eluted with 0.2% TFA and desalted using Sep-Pak tC18 (Waters) with 0.1% TFA in 28% ACN and ZipTip U-C18 (Millipore) with 1% FA in 50% ACN. The sample was dried by vacuum centrifugation and resuspended in 5% ACN with 0.1% TFA.

The sample was loaded into a nano-flow liquid chromatography (Easy-nLC 1000 system, Thermo) online-coupled to an Orbitrap mass spectrometer equipped with a nanospray ion source (Q Exactive Plus, Thermo). Nano-flow LC separation was performed with a linear gradient ranging from 3% to 30% buffer B (100% ACN and 0.1% FA) at a flow rate of 300 nL/min for 80 min using a 75  $\mu$ m  $\times$  20 cm capillary column with a particle size of 3  $\mu$ m (NTCC-360, Nikkyo Technos). For MS, survey scan spectra were acquired at a resolution of 70,000 at 200 m/z with an AGC target value of 3e6 ions and a maximum IT of 100 ms, ranging from 350 to 2000 m/z with charge states between 1+ and 4+. A data-dependent top 10 method was employed. The MS/MS resolution was 17,500 at 200 m/z with an AGC target value of 1e5 ions and a maximum IT of 120 ms.

### 4.3. MS Database Search for Cryptic Peptides

For the MS database search for cryptic peptides and canonical MHC ligands, we built a customized reference FASTA database, which contained every translation product derived from all possible ORFs found in the transcripts registered in the GENCODE database (v. M22). Possible ORFs were defined as sequences that began from the ATG codon and ended with stop codons or reached the transcript end, yielding polypeptides that were at least seven amino acids in length. Experimental MS/MS data were searched against the database using the Sequest HT and Percolator algorithms on the Proteome Discoverer 2.3 platform (Thermo). For database searching, the tolerance for precursor and fragment ions was set at 10 ppm and 0.02 Da, respectively. The oxidation of methionine (+15.995 Da) was selected as a dynamic modification. No specific enzyme was selected. For the subsequent analysis using Percolator (Thermo), concatenated target-decoy selection was validated based on the q-values. Annotated peptide spectrum matches (PSMs) with the highest score

(delta correlation ( $\Delta C_n$ )  $\leq 0.05$ ) were selected for each MS spectrum. We applied a false discovery rate (FDR) of 0.01 as the detection threshold. Identified sequences with a length of 8–11 amino acids,  $IC_{50} < 5000$  nM (H-2D<sup>d</sup>, NetMHC4.0), and source gene TPM > 0 in CT26 cells, were considered H-2D<sup>d</sup> ligands. The identified H-2D<sup>d</sup> ligand sequences were classified as either canonical or cryptic, according to their presence or absence in the mouse UniProtKB database (downloaded on 13 February 2020). During the comparison, every Ile was converted into Leu, as they are indistinguishable by MS.

#### 4.4. Synthetic Peptides

Synthetic peptides (MGPPRAAGI, 1110038B12Rik-MI9; AGPVAVSRF, Spr-AF9; QGP-DRGGDSL, Ss18l2-QL10; HGPRLEISL, Ythdf3-HL9; SGPARAWGV, Poli-SV9; SGPSRLYLL, Rpl3-SL9; TGPVVRGLSVF, Sdhd-TF10; QPARYFGF, Paics-QF8; SVPRRHVSF, Phlda3-SF9; RGPERSSEETVF, Plagl2-RF11; SGPLRGAGE, Lonp1-SF9; SGPERHVFV, Mrps18b-SV9; VGP-PRATVL, Ndr1-VL9; SGPRSIYIL, Kcnb1-SL9; LGPARSPSSF, Lig4-LF10; RGPVAGAVGL, Lonp1-RL10; QGPMALRLF, Cioa2a-QF9; SGPSRWKHQM, Ephx1-SM10; TGPQRNVCL, Ip6k1-TL9) with >80% purity were purchased (Cosmo Bio).

#### 4.5. RNA Sequencing (RNA-Seq)

Total RNA was isolated from CT26 cells using TRIzol reagent (Invitrogen). Library preparation and sequencing were performed by Macrogen (Tokyo, Japan). Briefly, poly A-selected libraries were prepared using the TruSeq Stranded mRNA LT Sample Prep Kit (Illumina), and were sequenced on NovaSeq 6000 (Illumina) with 40 M of 100-bp paired-end reads per sample. Read quality was validated, low-quality reads, adaptor sequences, contaminant DNA, and PCR duplicates were removed using FastQC (v0.11.7) and Trimmomatic (v0.38). The reads were mapped to the mouse reference genome (mm10) using HISAT2 (v2.1.0) and Bowtie2 (v2.3.4.1). The abundance of genes or transcripts was calculated as TPM using StringTie (v2.1.3b).

#### 4.6. Peptide Vaccination of Mice

BALB/c AJcl mice were purchased from Hokudo (Sapporo, Japan). Mice were maintained in the animal facility of Sapporo Medical University and all procedures were performed in accordance with the institutional animal care guidelines. Mice were subcutaneously immunized twice with 100  $\mu$ g Poly (I:C) (InvivoGen) containing 50  $\mu$ g each of synthetic cryptic peptides, or 100  $\mu$ g Poly (I:C) alone before CT26 injection (Days -10 and -3). Mice were then subcutaneously injected with  $1.0 \times 10^6$  CT26 cells in a mixture of saline and Matrigel Matrix (Corning) (Day 0), followed by a third immunization with 100  $\mu$ g Poly (I:C) containing peptides, or Poly (I:C) alone (Day 4). Tumor sizes were calculated as  $xy^2/2$ , where x and y represent the major and minor tumor axes, respectively, every 2–3 days. The endpoint was set as the major axis of 20 mm.

**Supplementary Materials:** The following are available online at <https://www.mdpi.com/article/10.3390/immuno1040030/s1>, Figure S1: Vaccination with cryptic peptides and the growth of CT26 cells in vivo.

**Author Contributions:** S.T. performed the experiments, analyzed the data, and wrote the manuscript. T.K. conceived and designed the study and wrote the manuscript. T.T. supervised the project. All authors reviewed and approved the contents of the manuscript. All authors have read and agreed to the published version of the manuscript.

**Funding:** This work was supported by the Japan Agency for Medical Research and Development (AMED) Grant to T.K. (JP21cm0106352), Grant-in-Aid for Scientific Research from the Japan Society for the Promotion of Science (JSPS) KAKENHI to T.K. (JP19H03490 and JP20K21528), AMED Grant to T.T. (JP20cm0106309), and JSPS KAKENHI to T.T. (JP17H01540).

**Institutional Review Board Statement:** The study was conducted with the approval of the Animal Study Committee of Sapporo Medical University (20-087).

**Informed Consent Statement:** Not applicable.

**Data Availability Statement:** MS raw data and FASTA files have been deposited to the ProteomeX-change Consortium via the jPOSTrepo partner repository (<https://repository.jpostdb.org>) with the dataset identifier PXD029094.

**Conflicts of Interest:** T.K. received grant support from Astellas. T.T. received grant support from Ono Pharmaceutical and Sumitomo Dainippon Pharma.

## References

1. Le, D.T.; Durham, J.N.; Smith, K.N.; Wang, H.; Bartlett, B.R.; Aulakh, L.K.; Lu, S.; Kemberling, H.; Wilt, C.; Luber, B.S.; et al. Mismatch-repair deficiency predicts response of solid tumors to PD-1 blockade. *Science* **2017**, *357*, 409–413. [[CrossRef](#)] [[PubMed](#)]
2. Gubin, M.M.; Zhang, X.; Schuster, H.; Caron, E.; Ward, J.P.; Noguchi, T.; Ivanova, Y.; Hundal, J.; Arthur, C.D.; Krebber, W.J.; et al. Checkpoint blockade cancer immunotherapy targets tumour-specific mutant antigens. *Nature* **2014**, *515*, 577–581. [[CrossRef](#)] [[PubMed](#)]
3. Hirama, T.; Tokita, S.; Nakatsugawa, M.; Murata, K.; Nannya, Y.; Matsuo, K.; Inoko, H.; Hirohashi, Y.; Hashimoto, S.; Ogawa, S.; et al. Proteogenomic identification of an immunogenic HLA class I neoantigen in mismatch repair-deficient colorectal cancer tissue. *JCI Insight* **2021**, *6*. [[CrossRef](#)] [[PubMed](#)]
4. Tran, E.; Robbins, P.F.; Lu, Y.C.; Prickett, T.D.; Gartner, J.J.; Jia, L.; Pasetto, A.; Zheng, Z.; Ray, S.; Groh, E.M.; et al. T-Cell Transfer Therapy Targeting Mutant KRAS in Cancer. *N. Engl. J. Med.* **2016**, *375*, 2255–2262. [[CrossRef](#)] [[PubMed](#)]
5. Neeffjes, J.; Jongsma, M.L.; Paul, P.; Bakke, O. Towards a systems understanding of MHC class I and MHC class II antigen presentation. *Nat. Rev. Immunol.* **2011**, *11*, 823–836. [[CrossRef](#)] [[PubMed](#)]
6. Rock, K.L.; Reits, E.; Neeffjes, J. Present Yourself! By MHC Class I and MHC Class II Molecules. *Trends Immunol.* **2016**, *37*, 724–737. [[CrossRef](#)] [[PubMed](#)]
7. Yewdell, J.W. DRiPs solidify: Progress in understanding endogenous MHC class I antigen processing. *Trends Immunol.* **2011**, *32*, 548–558. [[CrossRef](#)] [[PubMed](#)]
8. Starck, S.R.; Shastri, N. Non-conventional sources of peptides presented by MHC class I. *Cell Mol. Life Sci.* **2011**, *68*, 1471–1479. [[CrossRef](#)] [[PubMed](#)]
9. Laumont, C.M.; Daouda, T.; Laverdure, J.P.; Bonneil, E.; Caron-Lizotte, O.; Hardy, M.P.; Granados, D.P.; Durette, C.; Lemieux, S.; Thibault, P.; et al. Global proteogenomic analysis of human MHC class I-associated peptides derived from non-canonical reading frames. *Nat. Commun.* **2016**, *7*, 10238. [[CrossRef](#)] [[PubMed](#)]
10. Erhard, F.; Dolken, L.; Schilling, B.; Schlosser, A. Identification of the cryptic HLA-I immunopeptidome. *Cancer Immunol. Res.* **2020**, *8*, 1018–1026. [[CrossRef](#)] [[PubMed](#)]
11. Chong, C.; Muller, M.; Pak, H.; Harnett, D.; Huber, F.; Grun, D.; Leleu, M.; Auger, A.; Arnaud, M.; Stevenson, B.J.; et al. Integrated proteogenomic deep sequencing and analytics accurately identify non-canonical peptides in tumor immunopeptidomes. *Nat. Commun.* **2020**, *11*, 1293. [[CrossRef](#)] [[PubMed](#)]
12. Laumont, C.M.; Vincent, K.; Hesnard, L.; Audemard, E.; Bonneil, E.; Laverdure, J.P.; Gendron, P.; Courcelles, M.; Hardy, M.P.; Cote, C.; et al. Noncoding regions are the main source of targetable tumor-specific antigens. *Sci. Transl. Med.* **2018**, *10*. [[CrossRef](#)] [[PubMed](#)]
13. Kikuchi, Y.; Tokita, S.; Hirama, T.; Kochin, V.; Nakatsugawa, M.; Shinkawa, T.; Hirohashi, Y.; Tsukahara, T.; Hata, F.; Takemasa, I.; et al. CD8(+) T-cell Immune Surveillance against a Tumor Antigen Encoded by the Oncogenic Long Noncoding RNA PVT1. *Cancer Immunol. Res.* **2021**. [[CrossRef](#)] [[PubMed](#)]
14. Haen, S.P.; Loffler, M.W.; Rammensee, H.G.; Brossart, P. Towards new horizons: Characterization, classification and implications of the tumour antigenic repertoire. *Nat. Rev. Clin. Oncol.* **2020**, *17*, 595–610. [[CrossRef](#)] [[PubMed](#)]
15. Starck, S.R.; Shastri, N. Nowhere to hide: Unconventional translation yields cryptic peptides for immune surveillance. *Immunol. Rev.* **2016**, *272*, 8–16. [[CrossRef](#)] [[PubMed](#)]
16. Rosenthal, R.; Cadieux, E.L.; Salgado, R.; Bakir, M.A.; Moore, D.A.; Hiley, C.T.; Lund, T.; Tanic, M.; Reading, J.L.; Joshi, K.; et al. Neoantigen-directed immune escape in lung cancer evolution. *Nature* **2019**, *567*, 479–485. [[CrossRef](#)] [[PubMed](#)]